

UNSTEADY AERODYNAMIC WAKE OF HELICOPTER MAIN-ROTOR-HUB
ASSEMBLY

ISKANDAR SHAH BIN ISHAK

UNIVERSITI TEKNOLOGI MALAYSIA

UNSTEADY AERODYNAMIC WAKE OF HELICOPTER MAIN-ROTOR-HUB
ASSEMBLY

ISKANDAR SHAH IN ISHAK

A thesis submitted in fulfilment of the
requirements for the award of the degree of
Doctor of Philosophy (Mechanical Engineering)

Faculty of Mechanical Engineering
Universiti Teknologi Malaysia

JUNE 2012

*To my beloved parents (Haji Ishak and Hajah Aminah), wife (Norhayati) and
children (Izzati, Imran and Ikhmal)*

ABSTRACT

The helicopter tail shake phenomenon is an area of great concern to helicopter manufacturers as it adversely affects the overall performance and handling qualities of the helicopter, and the comfort of its occupants. This study is intended to improve the understanding of the unsteady aerodynamic load characteristics triggered by the helicopter main-rotor-hub assembly wake that lead to this phenomenon by experimental and numerical investigations. In this research work, a simplified NASA standard fuselage model was mated to a main-rotor-hub assembly from a remote-control helicopter. Data of pressures and velocities inside the wake, as well as the aerodynamic drag, corresponding to the variations of helicopter's advance ratios and pylon configurations were captured. This work had gained some useful information towards further understanding of this long running issue, with a potential to minimise the problem. The dynamic analysis, through the power spectral density, root-mean-square and probability density function analyses, was also conducted and had successfully quantified the frequency and unsteadiness of main-rotor-hub assembly wake. Computational Fluid Dynamics (CFD) had also been carried out to model and simulate the wake dynamics, and were successfully validated using experimental results. The Sliding Mesh method was opted to simulate the rotation of main-rotor-hub assembly whilst the aerodynamic flow field was computed using the Large Eddy Simulation equations. As the CFD results were found to be in accordance with the experimental results, a reliable CFD modelling technique for the unsteady wake analysis of the helicopter main-rotor-hub assembly wake has thus been forwarded. Accordingly, this numerical modelling could be used to supplement experimental work. In addition, this research programme had also successfully proposed a modelling technique of simplified helicopter main-rotor-hub assembly viable for unsteady aerodynamic wake studies.

ABSTRAK

Fenomena getaran pada ekor helikopter merupakan suatu isu yang dipandang berat oleh para pengeluar helikopter kerana ia memberi kesan kepada prestasi keseluruhan dan kualiti kawalan helikopter, serta keselesaan penumpang. Kajian ini bertujuan untuk menambahkan lagi kefahaman ke atas ciri keracak aerodinamik tidak-tetap dari hab-rotor-utama helikopter yang merupakan sumber utama penyebab fenomena ini, melalui kerja-kerja penyelidikan secara ujikaji dan simulasi berkomputer. Model fiuslaj piawai NASA yang dipermudah digandingkan bersama hab-rotor-utama dari helikopter kawalan jauh untuk digunakan sebagai model kajian. Data tekanan dan halaju dalam keracak, serta daya seret aerodinamik pada pelbagai nilai nisbah-maju dan konfigurasi pelindung hab-rotor-utama helikopter, telah diperolehi. Kajian yang dijalankan ini telah berjaya memberikan beberapa maklumat berguna yang mungkin berpotensi untuk mengurangkan permasalahan yang telah berlanjutan sekian lama ini. Analisis dinamik, menerusi analisis terhadap ketumpatan spektra kuasa, punca min kuasa dua dan fungsi ketumpatan kebarangkalian, juga dilakukan dan berjaya mengenalpasti frekuensi serta ketidak-tetapan aliran keracak hab-rotor-utama helikopter. Simulasi dinamik bendalir berkomputer juga dilakukan untuk memodelkan dan mensimulasikan dinamik keracak dan telah berjaya di tentusahkan dengan keputusan ujikaji. Kaedah Jejaring Gelangsar diaplikasikan untuk mensimulasikan putaran hab-rotor-utama helikopter manakala medan aliran aerodinamik dikira menggunakan persamaan Simulasi Olakan Besar. Oleh kerana hasil simulasi ini sejajar dengan keputusan ujikaji, suatu teknik permodelan simulasi untuk analisis keracak tidak-tetap hab-rotor-utama helikopter telah berjaya dihasilkan. Justeru itu, simulasi berkomputer ini juga boleh digunakan untuk melengkapkan lagi kerja ujikaji. Di samping itu, penyelidikan ini juga telah berjaya mencadangkan satu model bagi hab-rotor-utama helikopter dipermudah yang boleh digunakan bagi kajian keracak aerodinamik tidak-tetap.

TABLE OF CONTENTS

CHAPTER	TITLE	PAGE
	DECLARATION	ii
	DEDICATION	iii
	ABSTRACT	iv
	ABSTRAK	v
	TABLE OF CONTENTS	vi
	LIST OF TABLES	x
	LIST OF FIGURES	xii
	LIST OF SYMBOLS	xx
	LIST OF APPENDICES	xxii
1	INTRODUCTION	1
	1.1 Overview of Helicopter Tail Shake Phenomenon	1
	1.2 The Needs of Vertical Tail	3
	1.3 Review of Previous Related Tests	5
	1.4 Research Key Area	6
	1.5 Problem Statement	7
	1.6 Objective of the Research Program	8
	1.7 Scope of Work	8
2	METHODOLOGY	9
	2.1 Introduction	9
	2.2 Flight Parameters	9
	2.2.1 Rotor Advance Ratio, μ	10
	2.2.2 Angle of Attack, α	11

2.2.3	Yaw Angle , ψ	13
2.3	Wind Tunnel Model	13
2.3.1	Blade-stubs Configuration	14
2.4	Data Acquisitions	15
2.4.1	Type of Data Collections	15
2.4.2	Data Sampling	17
2.5	Simulation Works	18
2.6	Data Analysis	19
2.7	Scaling Issue	21
2.8	Flow Chart of Research Methodology	22
3	LITERATURE REVIEWS	23
3.1	Introduction	23
3.2	Helicopter Aerodynamic Flow Field	24
3.3	Previous Experimental Related Tests	25
3.4	Computational Works	30
4	DEVELOPMENT OF EXPERIMENTAL RIG	33
4.1	Introduction	33
4.2	Description of the Tunnel	33
4.3	Development of the Wind Tunnel Model	34
4.3.1	Ellipsoidal Fuselage	34
4.3.2	Main-rotor-hub Assembly	35
4.3.3	Pylon	36
4.4	Development of the Measurement Apparatus	37
4.4.1	KULITE Miniature Dynamic Pressure Transducer XCL-072	37
4.4.2	Wake Pressure Rake	38
4.4.3	DANTEC Constant Temperature Anemometers (CTA)	40
4.4.4	Hotwire Anemometer Tube Holder	41
4.4.5	Development of RPM Sensor	41
4.4.6	Instrumentations and Data Acquisition	42
4.5	Pre-experimental Works	43

4.5.1	Calibration of KULITE Dynamic Pressure Transducer	43
4.5.2	Calibration of DANTEC Hotwire Anemometer	46
5	EXPERIMENTAL WORKS	48
5.1	Introduction	48
5.2	Test Configurations	48
5.3	Data Collections	52
5.3.1	Total Pressure Measurements	52
5.3.2	Velocity Fluctuation Measurements	54
5.3.3	Aerodynamic Drag Load Measurement	54
6	RESULTS AND DISCUSSION	56
6.1	Introduction	56
6.2	Designation of Point Measurements	56
6.3	Angle of Attack for the Investigation	59
6.4	Contour Plots of C_{p_0} and the RMS of C_{p_0}	61
6.5	Dynamic Analysis	77
6.5.1	PSD, RMS and PDF Analysis of Pressure Data	77
6.5.2	PSD, RMS and PDF Analysis of Velocity Data	95
6.6	Repeatability Analysis	104
6.7	Correlation with Aerodynamic Drag Load	109
7	COMPUTATIONAL FLUID DYNAMIC MODELLING	120
7.1	Introduction	120
7.2	Domain Set-Up	121
7.3	Physical Model	121
7.4	Moving Mesh Method	122
7.5	Methodology	122
7.5.1	Mesh Elements	122
7.5.2	Axes of Rotation	123
7.5.3	Grid Independence Analysis	125
7.5.4	Description of Case Studies	128

7.6	Results And Discussion	128
7.6.1	Dynamic Analysis	143
7.7	Simplified Main-Rotor-Hub Assembly Model	149
7.7.1	A Two-blade-stubs Configuration	149
7.7.2	A Three-blade-stubs Configuration	154
8	CONCLUSIONS AND RECOMMENDATIONS	161
8.1	Concluding Remarks	161
8.1.1	Helicopter Advance Ratio, μ	163
8.1.2	Frequency of Main-Rotor-Hub Assembly Wake	163
8.1.3	Pylon Configurations	164
8.1.4	CFD Modelling And Simulation	165
8.2	Suggestions for Further Works	165
	REFERENCES	167
	Appendices A - F	173-191

LIST OF TABLES

TABLE NO	TITLE	PAGE
2.1	Helicopter Advance Ratios	10
4.1	Balance Load Ranges	34
5.1a	Test configuration without pylon	50
5.1b	Test configuration with an ellipsoidal pylon (single height)	50
5.1c	Test configuration with a rectangular pylon (single height)	51
5.1d	Test configuration with an ellipsoidal pylon (double height)	51
5.1e	Test configuration with a rectangular pylon (double height)	51
6.1	C_{p0} at various angle of attack	60
6.2	PSD for each pylon configurations for Point M7	81
6.3	RMS for each pylon configurations for Point M7	83
6.4	PSD energy reduction on Point M7 for $\mu = 0.35$	86
6.5	RMS reduction on Point M7 for $\mu = 0.35$	86
6.6	PSD energy reduction on Point L7 for $\mu = 0.35$	86
6.7	RMS reduction on Point L7 for $\mu = 0.35$	87
6.8	PSD energy reduction for Point M7 at the hub's wake frequency	88
6.9	RMS fluctuation reduction for Point M7 at the hub's wake frequency	89
6.10	PSD energy reduction on Point M7 at $\mu = 0.35$	96
6.11	RMS fluctuation reduction on Point M7 at $\mu = 0.35$	97
6.12	RMS values on Point M10 for No Pylon Configuration	102
6.13	Simulation works on No Pylon Configuration for the same advance ratio	103
6.14	$RMS_{C_{p0}}$ at Point M10 for various pylon configurations at $\mu = 0.35$	103

6.15	RMS _{Velocity} at Point M10 for various pylon configurations at $\mu=0.35$	104
6.16	RMS at Point M10 for various pylon configurations at $\mu = 0.41$	104
6.17	Case studies for the repeatability analysis	105
6.18	Repeatability analysis of the mean total pressure readings and its rms	105
6.19	Repeatability analysis of the mean velocity readings and its rms	105
6.20	Repeatability of dynamic analysis of pressure readings	106
6.21	Repeatability of dynamic analysis of velocity readings	106
6.22	$\% \Delta$ for no pylon configuration at $\Omega = 1400$ rpm	116
7.1	Number of meshing elements for Big Volume	125
7.2	Number of meshing elements for Small Volume	126
7.3	P_o at different rpm at No Pylon Configuration	130
7.4	Maximum P_o from experimental work	131
7.5	Comparison of the mean velocity at $\mu = 0.35$ ($V_\infty = 20 \text{ ms}^{-1}$)	131
7.6	ΔP_o at $\mu = 0.35$	132
7.7	Maximum local velocity at the free stream of 20 ms^{-1}	134
7.8	Vortex strength at $\mu = 0.35$	137
7.9	Comparison of the maximum values	142
7.10	Comparison of the minimum values	142
7.11	ΔC_{p_o} comparison	142
7.12	$\% \Delta$ Reduction on Point M7 at $\mu=0.35$	145
7.13	$\% \Delta$ Reduction of total pressure's energy and its fluctuation	153
7.14	Comparison of PSD reduction at $\mu=0.35$	156

LIST OF FIGURES

FIGURE NO	TITLE	PAGE
1.1	Schematic of tail shake phenomenon	2
1.2	Vibrations in the cockpit	2
1.3	Torque effect on a helicopter	3
1.4	MD Helicopters 520N NOTAR	4
1.5	Helicopter Directional Stability	5
1.6	Helicopter main-rotor-hub assembly	7
2.1	Schematic diagram of rotor hub wake's trajectories	12
2.2	Helicopter at yawed	13
2.3	Blade-stubs Configuration	15
2.4	Flow Chart of Data Analysis	21
2.5	Flow Chart for Research Methodology	22
3.1	Aerodynamic flow field of helicopter	24
3.2	Distribution of total pressure coefficient at $\mu = 0.20$	26
3.3	Wind tunnel test at Marignane tunnel	27
3.4	Before modification on fairing/pylon	27
3.5	After modification on fairing/pylon	28
3.6	Wind tunnel test at DNW - LST	28
3.7	Wind tunnel test at UTM-LST	29
4.1	An ellipsoidal fuselage	35
4.2	Single main rotor design in blade-stubs configuration	35
4.3	The ellipsoidal and rectangular pylons	36
4.4	Pylons with height of 35mm	37
4.5	KULITE XCL-072 Miniature Dynamic Pressure Transducer	37
4.6	Influence of tube length on total pressure data	38

4.7	Schematic diagram of wake pressure rake	39
4.8	The wake pressure rake at UTM tunnel	39
4.9	Single hot-wire type 55P01	40
4.10	Hotwire anemometer's tube holder	41
4.11	Schematic diagram of rotor rpm measurement	42
4.12	National Instruments 9237 Modules	43
4.13	Schematic diagram of Pressure Transducer Calibration	44
4.14	Calibration graph of a KULITE transducer	45
4.15	Repeatability Test	45
4.16	Hysteresis Test	46
4.17	Hotwire calibration in the process	47
4.18	Repeatability Test	47
5.1	Schematic layout of Universiti Teknologi Malaysia's wind Tunnel	48
5.2	Pylon configurations	50
5.3	Schematic diagram of total pressure mapping	52
5.4	Points of Measurement	53
5.5	Mapping of total pressure at zero angle of attack	53
5.6	Mapping of velocity at angle of attack -5°	54
5.7	Schematic diagram for drag load measurement	55
6.1	Points of Measurement	57
6.2	Schematic location of Point L7	57
6.3	Plane locations in the fraction of fuselage length	58
6.4	Schematic diagram of contour plot presentations for side plane	58
6.5	Schematic diagram of contour plot presentations for top plane	59
6.6	Distribution of C_{p0} at the front plane	60
6.7	Distribution of C_{p0} at left-side plane	62
6.8	Distribution of C_{p0} at mid-side plane	62
6.9	Distribution of C_{p0} at right-side plane	63
6.10	Distribution of C_{p0} at top plane ($z/fl = 0.244$)	63
6.11	Distribution of C_{p0} at top plane ($z/fl = 0.206$)	63
6.12	Distribution of $RMS_{C_{p0}}$ at right-side plane	64

6.13	Distribution of $RMS_{C_{p0}}$ at mid-side plane	64
6.14	Distribution of $RMS_{C_{p0}}$ at left-side plane	65
6.15	Distribution of $RMS_{C_{p0}}$ at top plane ($z/fl = 0.244$)	65
6.16	Distribution of $RMS_{C_{p0}}$ at top plane ($z/fl = 0.206$)	65
6.17	Distribution of $RMS_{C_{p0}}$ for No Pylon Configuration at $\mu = 0.62$	66
6.18	Distribution of $RMS_{C_{p0}}$ for Ellipsoidal Pylon (Single Height) Configuration at $\mu = 0.62$	66
6.19	Distribution of $RMS_{C_{p0}}$ for Rectangular Pylon (Single Height) Configuration at $\mu = 0.62$	67
6.20	Distribution of $RMS_{C_{p0}}$ for Ellipsoidal Pylon (Double Height) Configuration at $\mu = 0.62$	67
6.21	Distribution of $RMS_{C_{p0}}$ for 2 Rectangular Pylon (Double Height) Configuration at $\mu = 0.62$	68
6.22	Distribution of $RMS_{C_{p0}}$ for No Pylon Configuration at $\mu = 0.31$	68
6.23	Distribution of $RMS_{C_{p0}}$ for Ellipsoidal Pylon (Single Height) Configuration at $\mu = 0.31$	69
6.24	Distribution of $RMS_{C_{p0}}$ for Rectangular Pylon (Single Height) Configuration at $\mu = 0.31$	69
6.25	Distribution of $RMS_{C_{p0}}$ for Ellipsoidal Pylon (Double Height) Configuration at $\mu = 0.31$	70
6.26	Distribution of $RMS_{C_{p0}}$ for Rectangular Pylon (Double Height) Configuration at $\mu = 0.31$	70
6.27	Distribution of C_{p0} for No Pylon Configuration at $\mu = 0.62$	71
6.28	Distribution of C_{p0} for Ellipsoidal Pylon (Double Height) Configuration at $\mu = 0.62$	71
6.29	Distribution of C_{p0} for Rectangular Pylon (Double Height) Configuration at $\mu = 0.62$	72
6.30	Distribution of C_{p0} for No Pylon Configuration at $\mu = 0.31$	72
6.31	Distribution of C_{p0} for Ellipsoidal Pylon (Double Height) Configuration at $\mu = 0.31$	73
6.32	Distribution of C_{p0} for Rectangular Pylon (Double Height) Configuration at $\mu = 0.31$	73

6.33	Cp _o distribution at Point M7 (i.e. $x/fl = 0.25$ and $z/fl=0.168$)	74
6.34	RMS of Cp _o at Point M7	75
6.35	Point designations for No Pylon Configuration	75
6.36	Point designations for Ellipsoidal/Rectangular Pylon (Double Height) Configuration	75
6.37	Cp _o distribution at Point M8	76
6.38	Cp _o distribution at Point M9	76
6.39	RMS of Cp _o at Point M8	77
6.40	RMS of Cp _o at Point M9	77
6.41	PSD analysis at point M7 at $\Omega=1400$ rpm ($\mu=0.35$)	78
6.42	RMS analysis at point M7 at $\Omega=1400$ rpm ($\mu=0.35$)	79
6.43	PSD analysis for different pylon configurations at $\Omega=1400$ rpm ($\mu=0.35$)	80
6.45	RMS analysis for different pylon configurations at $\Omega=1400$ rpm ($\mu=0.35$)	82
6.46	RMS for different pylon configurations	83
6.47	PSD analysis for different pylon configurations at $\Omega= 1200$ rpm ($\mu=0.41$)	84
6.48	RMS analysis for different pylon configurations at $\Omega=1200$ rpm ($\mu=0.41$)	84
6.49	PSD analysis for different pylon configurations at $\Omega=1600$ rpm ($\mu=0.31$)	85
6.50	RMS analysis for different pylon configurations at $\Omega=1600$ rpm ($\mu=0.31$)	85
6.51	Schematic of flow path at various pylon configurations	90
6.52	PSD Analysis on Point M7 at the wake frequency	91
6.53	RMS Analysis on Point M7 at the wake frequency	91
6.54	PDF analysis on Point M7 for No Pylon Configuration at $\mu = 0.62$	92
6.55	PDF analysis on Point M7 for Ellipsoidal Pylon (Double Height) Configuration at $\mu = 0.62$	92
6.56	PDF analysis on Point M7 for Rectangular Pylon (Double Height) Configuration at $\mu = 0.62$	93

6.57	PDF analysis on Point M10 for No Pylon Configuration at $\mu = 0.41$	94
6.58	PDF analysis on Point M10 for Ellipsoidal Pylon (Double Height) Configuration at $\mu = 0.41$	94
6.59	PDF analysis on Point M10 for Rectangular Pylon (Double Height) Configuration at $\mu = 0.41$	95
6.60	PSD analysis on Point M7 for different pylon configurations at $\mu = 0.35$	96
6.61	PSD analysis on Point M7 for different hub's rpm	97
6.62	RMS analysis on Point M7 for different hub's rpm	98
6.63	PSD distribution on Point M7 at 20ms^{-1}	98
6.64	RMS distribution on Point M7 at 20ms^{-1}	99
6.65	PSD distribution on Point M7 at 20ms^{-1} (pressure measurement)	99
6.66	RMS distribution on Point M7 at 20ms^{-1} (pressure measurement)	100
6.67	PDF analysis on Point M10 for no pylon configuration at $\mu = 0.41$	100
6.68	PDF analysis on Point M10 for Ellipsoidal Pylon (Double Height) Configuration at $\mu = 0.41$	101
6.69	PDF analysis on Point M10 for Rectangular Pylon (Double Height) Configuration at $\mu = 0.41$	101
6.70	PDF analysis on Point M10 for various pylon configurations at $\mu = 0.41$	102
6.71	PSD repeatability analysis from two tests (pressure measurement)	107
6.72	RMS repeatability analysis from two tests (pressure measurement)	108
6.73	PSD repeatability analysis from two tests (velocity measurement)	108
6.75	Trends of aerodynamic drag coefficient	109
6.76	C_{p0} distribution at Point M7 (i.e. at the closest plane to rotor hub)	111
6.77	Aerodynamic drag coefficient at the lowest and	

	highest advance ratios	111
6.78	Aerodynamic characteristics for No Pylon Configuration	112
6.79	Aerodynamic characteristics at the lowest advance ratio, $\mu=0.31$	113
6.80	Aerodynamic characteristics at the highest advance ratio, $\mu=0.62$	113
6.81	RMS analysis at No Pylon configuration with $V_{\infty}=20 \text{ ms}^{-1}$	114
6.82	PSD analysis at no pylon configuration with $V_{\infty}=20 \text{ ms}^{-1}$	115
6.83	RMS analysis at no pylon configuration with $V_{\infty}=30 \text{ ms}^{-1}$	115
6.84	PSD analysis at no pylon configuration with $V_{\infty}=30 \text{ ms}^{-1}$	116
6.85	PSD analysis at $\mu = 0.41$ ($\Omega=1200 \text{ rpm}$)	117
6.86	RMS analysis at $\mu = 0.41$ ($\Omega=1200 \text{ rpm}$)	117
6.87	PSD analysis at $\mu = 0.35$ ($\Omega=1400 \text{ rpm}$)	118
6.88	RMS analysis at $\mu = 0.35$ ($\Omega=1400 \text{ rpm}$)	118
6.89	PSD analysis at $\mu = 0.31$ ($\Omega=1600 \text{ rpm}$)	118
6.90	RMS analysis at $\mu = 0.31$ ($\Omega=1600 \text{ rpm}$)	119
7.1	Meshing volume for high density mesh for No Pylon Configuration	123
7.2	Meshing volume for high density mesh for Ellipsoidal Pylon (Double Height) Configuration	123
7.3	Test section with model at $\alpha = -5^{\circ}$	124
7.4	Test section and model rotated upwards by 5°	124
7.5	The free stream is tilted to five degrees downwards	124
7.6	Grid independence analysis for the Big Volume	126
7.7	Grid independence analysis for the Small Volume	127
7.8	Path lines of total pressure (Pa) for No Pylon Configuration at $\mu = 0.31$ (side view)	128
7.9	Path lines of total pressure (Pa) for No Pylon Configuration at $\mu = 0.31$ (top view)	129
7.10	Path lines of total pressure (Pa) for No Pylon Configuration at $\mu = 0.35$ (side view)	129
7.11	Path lines of total pressure (Pa) for No Pylon Configuration at $\mu = 0.35$ (top view)	130
7.12	Path lines of total pressure (Pa) for Ellipsoidal Pylon	

	(Double Height) Configuration (side view)	132
7.13	Path lines of total pressure (Pa) for Ellipsoidal Pylon (Double Height) Configuration (top view)	132
7.14	Path lines of velocity (ms^{-1}) for No Pylon Configuration at $\mu = 0.31$ ($V_{\infty}=20 \text{ ms}^{-1}$ and $\Omega =1600 \text{ rpm}$)	133
7.15	Path lines of velocity (ms^{-1}) for No Pylon Configuration at $\mu = 0.35$ ($V_{\infty}=20 \text{ ms}^{-1}$ and $\Omega =1400 \text{ rpm}$)	134
7.16	Path lines of velocity (ms^{-1}) for Ellipsoidal Pylon (Double Height) Configuration at $\mu = 0.31$ ($V_{\infty}=20 \text{ ms}^{-1}$ and $\Omega =1600 \text{ rpm}$)	135
7.17	Path lines of velocity (ms^{-1}) for Ellipsoidal Pylon (Double Height) Configuration at $\mu = 0.35$ ($V_{\infty}=20 \text{ ms}^{-1}$ and $\Omega =1400 \text{ rpm}$)	135
7.18	Vortex at rotating zone for No Pylon Configuration	136
7.19	Vortex for No Pylon Configuration	136
7.20	Vortex at rotating zone for Ellipsoidal Pylon (Double Height) Configuration	137
7.21	Vortex for Ellipsoidal Pylon (Double Height) Configuration	137
7.22	Distribution of C_{p_o} at $\mu =0.31$ (Fluent)	138
7.23	Distribution of C_{p_o} at $\mu =0.35$ (Fluent)	138
7.24	Distribution of C_{p_o} at $\mu =0.31$ (Experimental)	139
7.25	Distribution of C_{p_o} at $\mu =0.35$ (Experimental)	139
7.26	Distribution of $\text{RMS}_{C_{p_o}}$ at $\mu = 0.31$ (Fluent)	140
7.27	Distribution of $\text{RMS}_{C_{p_o}}$ at $\mu = 0.35$ (Fluent)	140
7.28	Distribution of $\text{RMS}_{C_{p_o}}$ at $\mu = 0.31$ (Experimental)	141
7.29	Distribution of $\text{RMS}_{C_{p_o}}$ at $\mu = 0.35$ (Experimental)	141
7.30	PSD analysis on Point M7 at $\mu = 0.35$	143
7.31	RMS analysis on Point M7 at $\mu = 0.35$	144
7.32	PSD analysis on Point M7 at $\mu = 0.31$	144
7.33	RMS analysis on Point M7 at $\mu = 0.31$	145
7.34	PSD _{Velocity} analysis on M4 (at $V_{\infty}=20 \text{ ms}^{-1}$ and $\Omega=1400 \text{ rpm}$)	146
7.35	PSD _{Velocity} analysis on M5 (at $V_{\infty}=20 \text{ ms}^{-1}$ and	

	$\Omega=1400$ rpm)	146
7.36	RMS _{Velocity} analysis on M5 (at $V_\infty=20$ ms ⁻¹ and $\Omega=1400$ rpm)	147
7.37	PDF analysis on Point M10 for No Pylon Configuration	147
7.38	PDF analysis on Point M10 for Ellipsoidal Pylon (Double Height) Configuration	148
7.39	PDF analysis on Point M10 for No Pylon Configuration (Experimental)	148
7.40	PDF analysis on Point M10 for Ellipsoidal Pylon (Double Height) Configuration (Experimental)	149
7.41	A simplified main-rotor-hub assembly	150
7.42	Ortega simplified model of main-rotor-hub assembly	150
7.43	The simplified main-rotor-hub assembly mated to fuselage	151
7.44	The simplified main-rotor-hub assembly with pylon increased	151
7.45	RMS analysis at $V_\infty=20$ ms ⁻¹ and $\Omega=1400$ rpm	151
7.46	PSD analysis at $V_\infty=20$ ms ⁻¹ and $\Omega=1400$ rpm	152
7.47	RMS analysis at $V_\infty=20$ ms ⁻¹ and $\Omega=1600$ rpm	152
7.48	PSD analysis at $V_\infty=20$ ms ⁻¹ and $\Omega=1600$ rpm	153
7.49	A three-blade-stubs configuration	154
7.50	Model with the three-blade-stubs configuration	154
7.51	The simplified main-rotor-hub assembly with pylon height increased	154
7.52	RMS analysis at $\mu=0.35$	155
7.53	PSD analysis at $\mu=0.35$	155
7.54	RMS analysis at $\mu=0.31$	156
7.55	PSD analysis at $\mu=0.31$ ($V_\infty=20$ ms ⁻¹ and $\Omega=1600$ rpm)	157
7.56	RMS analysis at $\mu=0.35$ with MRF method	157
7.57	PSD analysis at $\mu=0.35$ with MRF method	158
7.58	Initial blades orientation	158
7.59	MRF at various flow times	159
7.60	Sliding Mesh at various flow times	159

LIST OF SYMBOLS

C_D	-	Aerodynamic drag coefficient
C_n	-	Yawing moment coefficient
C_{p_o}	-	Total pressure coefficient
$C_{p_o \text{ mean}}$	-	Mean total pressure coefficient
N	-	Number of data
P_∞	-	Free stream static pressure (Pa)
P_o	-	Total pressure (Pa)
q_∞	-	Free stream dynamic pressure (Pa)
R	-	Main rotor blade radius (m)
V_∞	-	Free stream or flight velocity (m/s)
β	-	Sideslip angle (deg)
Ω	-	Rotor rotation speed (radian/s)
μ	-	Helicopter rotor advance ratio
α	-	Angle of attack (deg)
γ	-	Incidence angle (deg)
ψ	-	Yaw angle (deg)

Abbreviations

CFD	-	Computational Fluid Dynamics
DNW-LST	-	German-Dutch Low Speed Tunnel
I/A	-	Interactional Aerodynamics
LabView	-	Laboratory Virtual Instrumentation Engineering Workbench
LES	-	Large Eddy Simulation
LDV	-	Laser Doppler Velocimetry
MRF	-	Multiple Reference Frames
NLR	-	National Aerospace Laboratory

NOTAR	-	No Tail Rotor
PSD	-	Power Spectral Density
PDF	-	Probability Density Function
RANS	-	Reynolds Averaged Navier-Stokes
RC	-	Remote Control
RMS	-	Root-Mean-Square
ROBIN	-	Rotor Body Interaction
UTM	-	Universiti Teknologi Malaysia

LIST OF APPENDICES

APPENDIX	TITLE	PAGE
A	Main-Rotor-Hub Assembly	173
B	More Results	174
C	Test Facility Background	185
D	Dimensions of Measurement Point Locations	189
E	Specifications of KULITE Dynamic Pressure Transducer	190
F	Hotwire Tube Holder	191

CHAPTER 1

INTRODUCTION

1.1 Overview of Helicopter Tail Shake Phenomenon

A helicopter is an aircraft that is lifted and propelled by one, or even more horizontal rotors, as is the case with the Boeing CH-47 Chinook, where each rotor consisting of two or more rotor blades.

The Interactional Aerodynamic (I/A) problems remain a long dragged issue in spite of numerous endeavours by a lot of companies (Waard and Trouvé, 1999). The statement is considerably supported by Hassan *et. al* (1999) which state the flow fields that govern the aircraft's handling qualities and responsiveness have often baffled designers. One of the critical I/A problems is the helicopter tail shake phenomenon that adversely affected the overall performance, occupant comfort and handling qualities of helicopter (Roesch and Dequin, 1983; Waard and Trouvé, 1999). According to Coton (2007), this phenomenon is a very complex problem and the European Helicopter Project (GO AHEAD) and French-Germany Project (SHANEL) are currently believed to look seriously at this phenomenon.

Essentially, the phenomenon occurs as a consequence of interaction between the unsteady main-rotor-hub assembly wake and the vertical tail of the helicopter (Coton, 2009), as be illustrated in Figure 1.1.

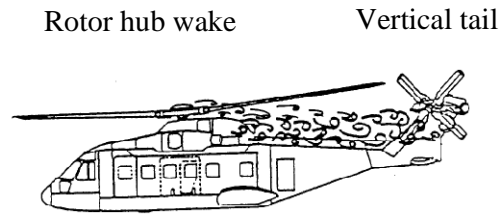


Figure 1.1: Schematic of tail shake phenomenon (Waard and Trouvé, 1999)

In fact, the phenomenon is a dynamic response of the structure to the main-rotor-hub assembly wake (Eurocopter, 2006). According to Roesch and Dequin (1983), with more new faster helicopter be developed and raise in mission requirements (Hassan *et al.*, 1999), the problems arising from the main-rotor-hub assembly's wake interactions with the tail surfaces have become more critical in such:

- (i) Additional drag and reduced performance due to the low energy wake triggered by the main-rotor-hub assembly's wake.
- (ii) Penalties to vehicle stability characteristics in pitch and yaw occur when the horizontal tail, vertical tail or tail rotor are surrounded by the highly unsteady wake. The effectiveness of stabilizer as well be degraded due to the dynamic pressure loss inside the wake.
- (iii) Unsteady flow components in the turbulent wake may cause structural buffeting of the tail surfaces. According to Waard and Trouvé (1999), these vibrations will be transmitted to cockpit and may deteriorate occupant comfort, as well adversely affect crew efficiency. Figure 1.2 illustrates the comfortless of the crew during tail shake phenomenon. Worked by Hassan *et al.* (1999) had also shared the same findings.

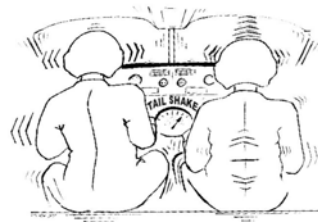


Figure 1.2: Vibrations in the cockpit (Waard and Trouvé, 1999)

- (iv) In the case of the frequency of main-rotor-hub assembly's wake coincides with a natural frequency of the tail parts, strong amplification of the vibration would occur. Consequently, premature structural failure may happen due to fatigue problem.

With these mentioned penalties, apparently extensive researches are much required to be done in this field in the hope to minimize the problems.

1.2 The Needs of Vertical Tail

Theoretically, the instant solution to this tail shake problem is to design a helicopter without the vertical tail. However, the vertical tail is required for two distinct purposes:

- (i) To house or mount the tail rotor - with a single main rotor helicopter, the creation of torque as the engine turns the rotor blades create a torque effect (Padfield, 1996) that causes the body of the helicopter to turn in the opposite direction of the rotor blades. Therefore, tail rotor is needed to produce yaw moment to compensate main rotor torque as be illustrated in Figure 1.3.

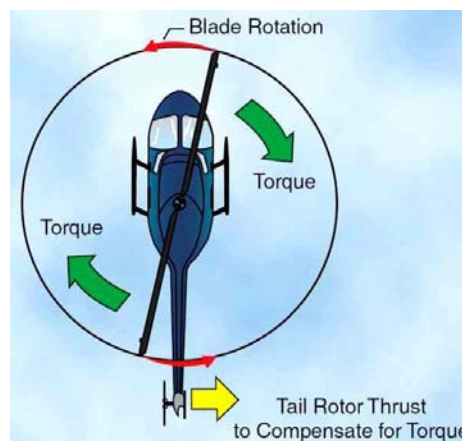


Figure 1.3: Torque effect on a helicopter (Google Images, 2011)

- (ii) For directional stability - in order to be statically stable in directional mode, the yawing moment derivative, Cn_β must be a positive value (Nelson, 1998).

Efforts had been made to replace tail rotor with different mechanisms that serve the same purpose. One of them is the NOTAR helicopter, an acronym for **NO TAIL Rotor** as shown in Figure 1.4, which is a relatively new helicopter anti-torque system that eliminates the use of the tail rotor on a helicopter. It uses jet thrusters to produce side force, and thus yaw moment to counter act the main motor torque.



Figure 1.4: MD Helicopters 520N NOTAR (Wikipedia, 2011)

Nevertheless, NOTAR helicopters still need to have vertical tail for its directional stability; consequently it is still being exposed to tail shake phenomenon. Works done by Ishak *et. al* (2008) on a generic 14% scaled-down model of Eurocopter 350Z helicopter had shown without the vertical tail, the helicopter would not be statically stable in directional mode as the yawing moment derivative, Cn_β becoming a negative value, as be demonstrated in Figure 1.5. It shows with the negative value of Cn_β , the helicopter deviates more from its initial equilibrium position. For the note, Cn is taken positive in clockwise direction looking from the top.

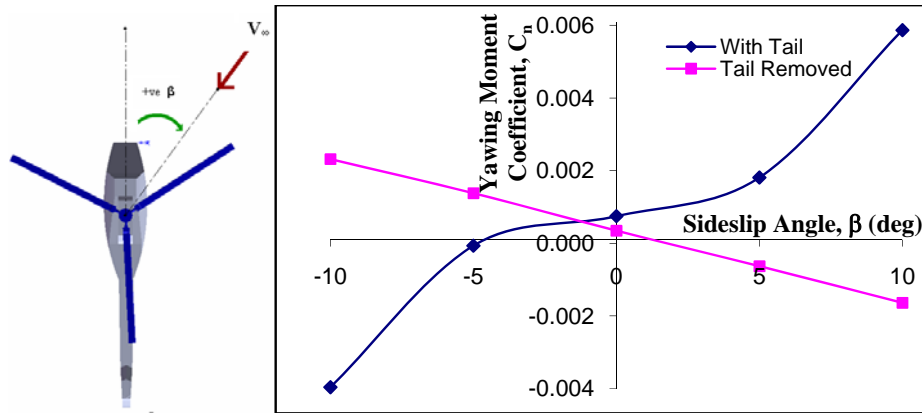


Figure 1.5: Helicopter Directional Stability (Ishak *et. al*, 2008)

This leads development of a helicopter which has neither vertical tail, nor tail rotor. It uses air-jet, positioned at the end of tail boom, for anti-torque and directional stability – this is made possible by adjusting the speed and amount of air jet in response of disturbance. However this kind of helicopter becomes very expensive and totally dependent on complex electronic control system, which its reliability could be an issue to some people.

For these highlighted reasons, new helicopter design still needs to be equipped with vertical tail assembly and thus, tail shake phenomenon issue is still relevant and needs to be addressed appropriately.

1.3 Review of Previous Related Tests

Previous researches such as Moedersheim and Leishman (1995) had done some total pressure measurements on the rotor wake but the advance ratios of the works were very low, which were only up to 0.3. Consequently the wake did not impinge on the empennage region. According to Sheridan (1979) and Ghee and Elliott (1995), the rotor hub wake can have a considerable influence on the flow environment in the vicinity of tail parts at high advance ratios. Therefore it is a need to do the investigations at higher advance ratios beyond 0.3, and this research aims to fulfil it.

Very little information on tail shake is available in the open literature because such information is commercially sensitive to manufacturers (Coton, 2009; Roesch and Dequin, 1983). There are only a few public papers on this subject and to make worst, some specific data and results are omitted to avoid being used by others. Hence, the information of these papers is not completed and could not straightly be used. As for instance, the chapter of tail shake test in Documentation Training (2006) provided by Eurocopter France to UTM-Aerolab is not furnished with the details of test configurations and data analysis - believed to be due to the confidential issues. Therefore it is hope that the open literature of this work can contribute literatures and thus benefit the rotorcraft community.

1.4 Research Key Area

As stated by Eurocopter (2007), the helicopter tail shake phenomenon is still not fully understood, justifying more researches to resolve this phenomenon. This work has shown merit as it manages to attract the Eurocopter France to assign one of its aerodynamicists to advice during the preliminary stage of the research.

Waard and Trouvé (1999) explain the helicopter tail shake phenomenon is being an interaction between the *aerodynamic excitation*, which is related to flight parameters, and the *structural response*, which is related to structure characteristics. As the aerodynamic excitation and structural response are two broadly diverse areas which are quite implausible to be covered in one merely PhD research, this study focused only on the aerodynamic excitation issue, in which works concentration will be on the hub wakes as it is believed to be the major contributor of the tail shake phenomenon (Cassier *et al.*, 1994; Hermans *et al.*, 1997; Eurocopter, 2007). Figure 1.6 illustrates the schematic diagram of the main-rotor-hub assembly where the hub wake is originated.

Main-rotor-hub Assembly

in Rotor

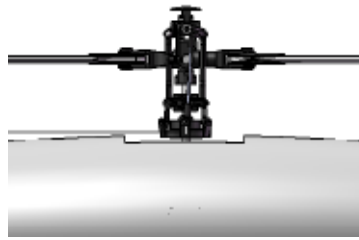


Figure 1.6: Helicopter main-rotor-hub assembly (inside the dotted-box)

The core analysis of this research work is to quantify the unsteadiness of helicopter's main-rotor-hub assembly wake with regards to the changes of flight parameters (i.e. the forward flight speed and main rotor rpm) and pylon configurations.

1.5 Problem Statement

Tail shake is very complex problem (Coton, 2007). It is one of the Interactional Aerodynamics (I/A) problems and remains, despite a considerable effort by different companies over the last two decades, difficult to predict with confidence before the first flight of a new helicopter (Waard and Trouvé, 1999). According to Eurocopter (2007), the helicopter tail shake phenomenon is an interesting problem to helicopters manufacturer but yet a very difficult subject to be understood.

As the helicopter main-rotor-hub assembly's wakes is believed to be the major contributor of the tail shake phenomenon (Cassier *et al.*, 1994; Hermans *et al.*, 1997; Eurocopter, 2007), this project will concentrate on the research of the unsteady aerodynamic characters triggered by helicopter's main-rotor-hub assembly wake. Moedersheim and Leishman (1995) had done some total pressure measurements on the rotor wake but the advance ratios of the works were only up to 0.3, which is too low for the hub wake to influence the flow environment in the vicinity of tail parts. Consequently it is a demand to do the investigations at higher advance ratios beyond

0.3, and this research aims to cater the demand and thus giving additional information and contribution.

1.6 Objective of the Research Program

The objective of this study is to improve the understanding of the unsteady aerodynamic loads characters triggered by the wake of the helicopter's main-rotor-hub assembly that lead to the helicopter tail shake phenomenon by proposing experimental and numerical investigations to gain useful information which has the potential to minimize the long dragged helicopter's tail shake problem.

1.7 Scope of Work

This study concentrates on the aerodynamic loads fluctuation of the unsteady main-rotor-hub assembly wake that leads to helicopter tail shake phenomenon.

The project needs to design and fabricate the appropriate experimental set-up, do the **Computational Fluid Dynamic (CFD)** modelling and simulation, develop the test procedure, instrumentations and data analysis that should be able to predict the unsteady aerodynamic loads fluctuation elicited by helicopter's main-rotor-hub assembly wake.

REFERENCES

- Berselli, L.C. *et al.* (2005). *Mathematics of Large Eddy Simulation of Turbulent Flows*. ISBN-13 978-3-540-26316-6 Springer Berlin Heidelberg New York.
- Boyd, D.D. and Barnwell, R.W. (2000). *A Computational Model for Rotor-Fuselage Interactional Aerodynamics*. AIAA Paper 2000-0256, AIAA 38th Aerospace Sciences Meeting & Exhibit, Reno NV, January 10-13 2000.
- Bradbrooke, F.D. (1972). *The World's Helicopters*. The Bodley Head Ltd. ISBN 0 370 01557 6. London.
- Brown, R.E. (2000). *Rotor Wake Modeling for Flight Dynamic Simulation of Helicopters*. AIAA Journal. Vol. 38, No 1, January 2000.
- Carpenter, P.J. and Fridovich, B. (1953). *Effect of a Rapid Blade-Pitch Increase on the Thrust and Induced Velocity Response of a Full-Scale Helicopter Rotor*. NACA TN 3044.
- Cassier, A. *et al.* (1994). *Aerodynamic development of the tiger helicopter*. 50th American Helicopter Society Forum, May 1994.
- Cosner, R.R. and Rahaim, C.P. (2001). *The AIAA Committee on Standard for CFD*. QNET-CFD Conference. Greece.
- Costes, M. *et al.* (2000). *Computational Tools Used at ONERA for the Description of Helicopter Rotor Wakes*. AIAA 2000-0113.

- Coton, F. (2011). *Email Conversation*. Professor of Low Speed Aerodynamics, Department of Aerospace Engineering, University of Glasgow.
- Coton, F. (2009). *Personal Discussion*. Professor of Low Speed Aerodynamics, Department of Aerospace Engineering, University of Glasgow.
- Coton, F. (2009). *Evaluation of UTM Research Projects*. Professor of Low Speed Aerodynamics, Department of Aerospace Engineering, University of Glasgow.
- Coton, F.N. *et al.* *Helicopter Tail Rotor Orthogonal Blade Vortex Interaction*. Department of Aerospace Engineering, University of Glasgow, Glasgow.
- De Waad, P.G. and Trouvé, M. (1999). *Tail shake vibration*. National Aerospace Laboratory (NLR), American Helicopter Society Annual Forum, May 1999.
- Deardorff, J.W. (1970). *A Numerical Study of Three-dimensional Turbulent Channel Flow at Large Reynolds Numbers*. J. Fluid Mech, 41(453-480).
- Elliot J.W., Althoff, S.L. and Sailey, R.H. (1988). *Inflow Measurements with a Laser Velocimeter on a Helicopter Model in Forward Flight; Volume I Rectangular Planform Blades at an Advance Ratio of 0.15*, NASA TM 100541, April 1988.
- Elliot J.W., Althoff, S.L. and Sailey, R.H. (1988). *Inflow Measurements with a Laser Velocimeter on a Helicopter Model in Forward Flight; Volume II Rectangular Planform Blades at an Advance Ratio of 0.23*, NASA TM 100542, April 1988.
- Elliot J.W., Althoff, S.L. and Sailey, R.H. (1988). *Inflow Measurements with a Laser Velocimeter on a Helicopter Model in Forward Flight; Volume III Rectangular Planform Blades at an Advance Ratio of 0.30*, NASA TM 100543, April 1988.
- Eurocopter France (2006). *Eurocopter Slide Presentation*.
- Eurocopter Marignane (2006). *UTM Malaysia Documentation Training*.

- Finn, E. (2001). *How to Measure Turbulence with Hot-wire Anemometers*. Dantec Dynamics A/S.
- Fluent (2005). *Introduction to GAMBIT - Training Notes*. Fluent Inc.
- Freeman, C.E. and Mineck, R.E. (1979). *Fuselage Surface Pressure Measurements of a Helicopter Wind-Tunnel Model With a 3.15-Meter Diameter Single Rotor*. NASA TM 80051, 1979.
- Ghee, T.A., Berry, J.D., Zori, L.A.J. and Elliot, J.W. (1996). *Wake Geometry Measurements and Analytical Calculations on a Small-Scale Rotor Model*. NASA TP 3584, August 1996.
- Ghee, T.A. and Elliot, J.W. (1995). *The Wake of a Small-Scale Rotor in Forward Flight Using Flow Visualization*. Journal of the American Helicopter Society. Volk. 40, (3).
- Hassan, A. *et al.* (1999). *Resolution of tail buffet phenomena for AH-64DTM Longbow ApacheTM*. Journal American Helicopter Society, Volume 44.
- Hermans, C. *et al.* (1997). *The NH90 helicopter development wind tunnel programme*. European Aerospace Societies Conference, Cambridge UK.
- Ishak, I.S. (2008). *PhD Proposal: Unsteady Aerodynamic Wake on Helicopter Tail Shake Phenomenon*. Universiti Teknologi Malaysia.
- Ishak, I.S., Mansor, S. and Mat Lazim, T. (2008). *Experimental Research On Helicopter Tail Shake Phenomenon*. Issue 26, Jurnal Mekanikal, pp. 107-118, ISBN 0127-3396, Universiti Teknologi Malaysia.
- Ishak, I.S. *et al.* (2008). *Mapping of Turbulence Intensity on Helicopter Model by Wind Tunnel Test*. The 1st International Meeting on Advances in Thermo-Fluids - IMAT'08, Johor, Malaysia, August 2008.

- Ishak, I.S. *et al.* (2008). *Experimental Research on Helicopter Tail Shake Phenomenon*. 2nd Regional Conference on Vehicle Engineering & Technology – RiVET’08, Kuala Lumpur, Malaysia, July 2008.
- Ishak, I.S. *et al.* (2008). *Wind Tunnel Test on a Generic Eurocopter 350Z Helicopter*. 2nd Regional Conference on Vehicle Engineering & Technology – RiVET’08, Kuala Lumpur, Malaysia, July 2008.
- Ishak, I.S. *et al.* (2008). *Preliminary Experimental Research on Helicopter Tail Shake Phenomenon*. Subsonic Aerodynamic Testing Association Conference – SATA’08, Pretoria, South Africa, June 2008.
- Ishak, I.S. *et al.* (2009). *Numerical Analysis of helicopter tail shake phenomenon : A Preliminary Study On Unsteady Wake*. 2nd International Conference on Engineering Technology 2009 - ICET’09, Kuala Lumpur, Malaysia.
- Ishak, I.S. *et al.* (2009). *Preliminary Numerical Analysis On Helicopter Main-Rotor-Hub-Assembly Wake*. The 2nd International Meeting on Advances in Thermo-Fluids - IMAT’09, Bogor, Indonesia, November 2009.
- Ishak, I.S. *et al.* (2009). *Numerical Analysis of helicopter tail shake phenomenon : A Preliminary Investigation*. The 2nd International Meeting on Advances in Thermo-Fluids - IMAT’09, Bogor, Indonesia, November 2009.
- Ishak, I.S. *et al.* (2010). *Computational Fluid Dynamic Studies On Helicopter Main-Rotor-Hub Assembly Wake*. Regional Conference On Mechanical And Aerospace Technology – RCMEAE, Bali, Indonesia.
- Kenyon, A.R. and Brown R.E. (2007). *Wake Dynamics and Rotor - Fuselage Aerodynamic Interactions*. American Helicopter Society 63rd Annual Forum.
- Kerr, A. (1975). *Effect of Helicopter Drag Reduction on Rotor Dynamic Loads and Blade Life*. Proceedings of the American Helicopter Society Symposium.

- Keys, C. N. and Rosenstein, H. J. (1978). *Summary of Rotor Hub Drag Data*. NASA CR-152080.
- Koushik, S.N. (2007). *A New Experimental Approach to Study Helicopter Blade-Vortex Interaction Noise*. PhD Thesis. University of Maryland.
- Lee, B.H.K. and Brown, D. (1990). *Wind Tunnel Studies of A F/A-18 Tail Buffet*. American Institute of Aeronautics and Astronautics, AIAA-90-1432.
- Mineck, R.E. and Althoff Gorton, S. (2000). *Steady and Periodic Pressure Measurements on a Generic Helicopter Fuselage Model in the Presence of a Rotor*, NASA TM 2000- 210286, June 2000.
- Nelson, R.C. (1998). *Flight Stability And Automatic Control*. 2nd Edition, McGraw-Hill International Editions.
- Ortega, F.T. *et al.* (2011). *Deconstructing Hub Drag*. American Institute of Aeronautics and Astronautics.
- Padfield, G.D. (1996). *Helicopter Flight Dynamics*. Blackwell Science Ltd.
- Padfield, G. (2007). *Email Conversation*, The University of Liverpool, United Kingdom.
- Park, Y.M., Nam and H.J. Kwon, O.J. (2006). *Simulation of Unsteady Rotor-Fuselage Interactions Using Unstructured Adaptive Meshes*. Journal of the American Helicopter Society. Vol. 51, No. 2, April 2006, pp. 141-149.
- Sheehy, T.W. and Clark, D. R. (1975). *A General Review of Helicopter Rotor Hub Drag Data*. 31 st Annual National Forum of the American, May 1975.
- Sheridan, P.F., and Smith, R.P. (1979). *Interactional Aerodynamics – A New Challenge to Helicopter Technology*. American Helicopter Society 35th Annual Forum, Washington DC.

- Sheridan, P.F., and Smith, R.P. (1980). *Interactional Aerodynamics – A New Challenge to Helicopter Technology*. Journal of the American Helicopter Society, Vol. 25, No. 1
- Stern, F. et al. (2001). *Comprehensive Approach to Verification And Validation of CFD Simulation - Part 1*. Journals of Fluids Engineering.
- Stern, F. et al. (2001). *Comprehensive Approach to Verification And Validation of CFD Simulation - Part 2*. Journals of Fluids Engineering.
- Sung, D.Y. et al. (1989). *An Experimental Investigation of Helicopter Rotor Hub Fairing Drag Characteristics*. NASA.
- Tyagi, M. (1995). Large Eddy Simulation of Complex Turbulent Flows. PhD Thesis. Indian Institute of Technology.